

Article

Effects of Climate Change and Fire on the Middle and Late Holocene Forest History in Yenisei Siberia

Elena Novenko ^{1,2}, Olga Rudenko ³, Natalia Mazei ², Dmitriy Kupriyanov ^{1,4}, Rodion Andreev ², Anton Shatunov ¹, Maria Kusilman ⁵, Anatoly Prokushkin ^{6,7} and Alexander Olchev ^{8,*}

- ¹ Department of Quaternary Paleogeography, Institute of Geography of the Russian Academy of Sciences, Staromonetny lane, 29, Moscow 119017, Russia; eynovenko@igras.ru or lenanov@mail.ru (E.N.); dmitriykupriyanov1994@yandex.ru (D.K.); toxavilli@yandex.ru (A.S.)
- ² Department of Physical Geography and Landscape Science, Faculty of Geography, Lomonosov Moscow State University, GSP–1, Leninskie Gory, 1, Moscow 119991, Russia; natashamazei@mail.ru (N.M.); dorionio40@gmail.com (R.A.)
- ³ Department of Geography, Ecology and General Biology, Orel State University Named After I.S. Turgenev, Komsomol'skaya Str., 95, Orel 302026, Russia; olrudenko2011@yandex.ru
- ⁴ Context Anthropology Laboratory, Institute of Archaeology of the Russian Academy of Sciences, Dmitriya Ulyanova St., 19, Moscow 117292, Russia
- ⁵ Department of Cartography and Geoinformatics, Faculty of Geography, Lomonosov Moscow State University, GSP–1, Leninskie Gory, 1, Moscow 119991, Russia; kusilman@rambler.ru
- ⁶ Laboratory of Biogeochemical Cycles in Forest Ecosystems, V.N. Sukachev Institute of Forest SB RAS, Federal Research Center "Krasnoyarsk Science Center SB RAS", Akademgorodok 50/28, Krasnoyarsk 660036, Russia; prokushkin@ksc.krasn.ru
- ⁷ School of Ecology and Geography, Siberian Federal University, Svobodny av., 79, Krasnoyarsk 660041, Russia
- ⁸ Department of Meteorology and Climatology, Faculty of Geography, Lomonosov Moscow State University, GSP–1, Leninskie Gory, 1, Moscow 119991, Russia
- * Correspondence: aoltche@yandex.ru or aoltche@gmail.com



Citation: Novenko, E.; Rudenko, O.; Mazei, N.; Kupriyanov, D.; Andreev, R.; Shatunov, A.; Kusilman, M.; Prokushkin, A.; Olchev, A. Effects of Climate Change and Fire on the Middle and Late Holocene Forest History in Yenisei Siberia. *Forests* **2023**, *14*, 2321. <https://doi.org/10.3390/f14122321>

Academic Editor: Federico Di Rita

Received: 5 October 2023

Revised: 19 November 2023

Accepted: 24 November 2023

Published: 26 November 2023



Copyright: © 2023 by the authors. Licensee MDPI, Basel, Switzerland. This article is an open access article distributed under the terms and conditions of the Creative Commons Attribution (CC BY) license (<https://creativecommons.org/licenses/by/4.0/>).

Abstract: This study presents the long-term forest history in the forest–tundra ecotone of the Low Yenisei River basin. The new high-resolution pollen and macroscopic charcoal data were inferred from the 8.6 m long peat archive covering the last 6300 years. Climate reconstructions are based on the application of the best modern analogue technique using pollen data. Our findings suggest an alternation of phases of middle-taiga forests of *Larix sibirica*, *Abies sibirica*, *Picea obovata*, and *Pinus sibirica* (intervals of climate warming: 6320–6050, 5790–5370, 4480–4220, and 3600–2700 cal yr BP, respectively) and open larch woodlands with the participation of *Betula*, *Picea*, and *Pinus sibirica*, typical for northern taiga (intervals of climate cooling and increasing humidification: 5370–4480, 4220–3600 cal yr BP, respectively). The vegetation pattern of the region became similar to the modern one around 2700 cal yr BP. Climate warming caused a northward shift of vegetation-zone boundaries in Yenisei Siberia and an expansion of the range of *Abies sibirica* by about 200 km to the north compared to the present day. The increased frequency of fires and biomass burning during warm periods may promote the melting of the local permafrost, thereby enhancing the tree growth and regeneration.

Keywords: pollen analysis; vegetation history; macroscopic charcoal; forest fire; paleoclimate; best modern analogue technique

1. Introduction

Current climate conditions are characterized by a steadily rising global temperature, changing precipitation patterns, and growing frequency and severity of extreme weather events [1]. High-latitude forest ecosystems have become highly vulnerable to environmental change in recent decades, as climate warming has been more pronounced in the high-latitude regions than in other parts of the world [2]. Rising air temperatures and more frequent heat waves with reduced precipitation are expected to increase drought conditions

and the risk of wildfires in the region [3,4]. These changes may also lead to permafrost degradation and shifts in vegetation patterns of tundra and forest biomes [5–9].

The palaeoecological reconstruction of the history of forests and fires in the past is crucial for a better understanding of the possible consequences of the current climate change for the forest ecosystems. Available Holocene paleoenvironmental reconstructions from various natural archives in the Arctic show a remarkable ecosystem response to past climate variability [10–17]. Especially for the area of northern Siberia, high regional variability in long-term vegetation and climate dynamics was revealed, with several phases of climate fluctuations. Paleoenvironmental reconstructions based on multiproxy records from the inner part of Siberia [18–23] showed a high sensitivity of forest ecosystems in Eastern and Western Siberia to Holocene climate changes. A close relationship between positive temperature anomalies and wildfire frequency was also shown [24–30]. However, despite their substantial contribution to our understanding of natural processes in the high-latitude regions, high-resolution palaeoecological records in northern Siberia are still very limited. Therefore, new studies are very important in this case to obtain more detailed information on possible mechanisms of climate–vegetation interaction in past epochs in the study region, thereby confirming or disproving previously formulated hypotheses.

Our present study of forest and fire history focuses on the forest area near the town of Igarka in Russia, located on the eastern margin of the West Siberian Lowlands in the Lower Yenisei River Basin. The plant cover of the various types of mires and the peat stratigraphy in the study area have been described by Katz [31] and Vasilchuk et al. [32]. The previous palynological and plant macrofossil records from this region were obtained by Piavchenko [33], Levkovskaya et al. [34], and Andreev and Klimanov [12].

In our paper, we introduce the novel high-resolution pollen and macroscopic charcoal data obtained from an 8 m long peat sequence covering the mid- to late-Holocene. The objectives of the study are: (1) to reconstruct the forest and fire history; (2) to reveal the relationships between vegetation change, wildfire frequency, and climate in the study area; and (3) to correlate our new findings with the Holocene climate change and environmental dynamics in the Russian Arctic.

2. Material and Methods

2.1. Study Area

The study area is located near the town of Igarka (Figure 1) in the Turukhansk district of the Krasnoyarsk region (Russia). The topography in this area is mostly flat to gently sloping, with low elevations ranging from 30 to 50 m above sea level. Abundant peatlands with perennial frost mounds are widespread.

The climate of the study area is subarctic, with prolonged and severe winters and short but relatively mild summers [35]. The mean annual air temperature is about -8.5 °C, and the mean temperatures of the coldest (January) and warmest (July) months are -28.9 °C and 15.6 °C, respectively [36]. Precipitation reaches 486 mm per year. The region belongs to the continuous permafrost area [37].

The study area belongs to the northern-taiga vegetation zone. The main forest forming trees are *Larix sibirica* Ledeb., *Picea obovata* Ledeb., *Betula pendula* Roth., and *Pinus sibirica* Du Tour. Our field observations showed the predominance of open larch, spruce-larch and pine-larch woodlands with a canopy density of 0.4–0.5 and extensive areas of early successional stands after clear-cutting and fires.

As a paleoarchive for the study of the Holocene forest and fire dynamics, we chose the peatland (hereafter Igarka peatland, $67^{\circ}31'53.77''$ N, $86^{\circ}38'05.65''$ E) situated about 10 km northeast of the town of Igarka (Figures 1 and 2). A detailed description of the peatland vegetation, the results of preliminary charcoal and plant macrofossil analysis and loss on ignition (LOI) measurements of the Igarka peat core, as well as the pollen and plant macrofossil records from the short peat core extracted from an unfrozen hollow near the study site have been published previously by Novenko et al. [38,39] and are used to discuss the palynological and macroscopic charcoal records presented here for the first time.

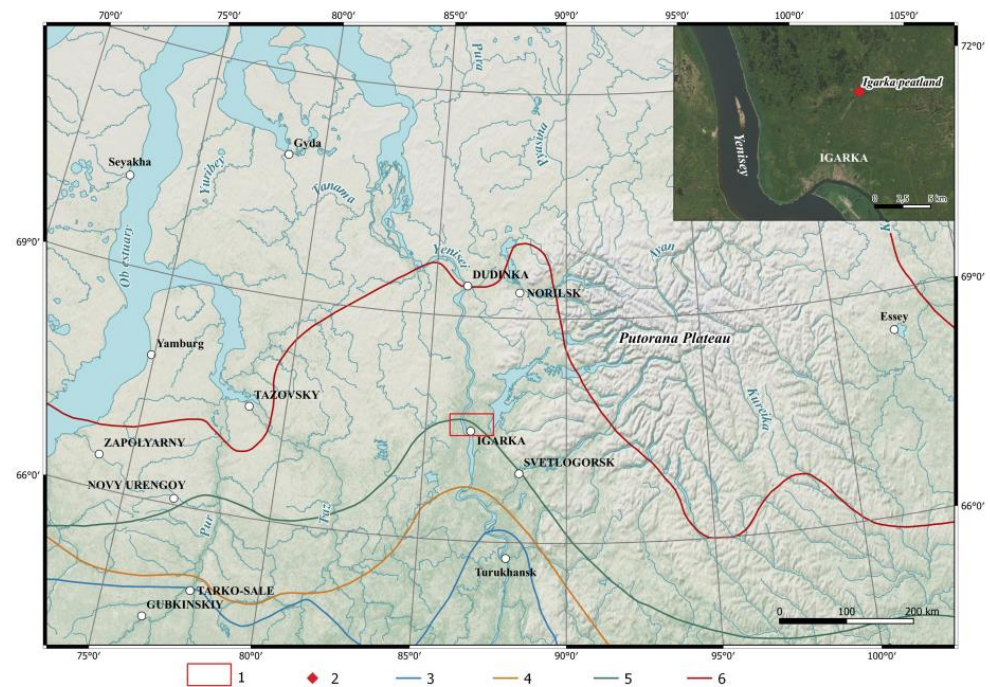


Figure 1. Location of the study area on the map of North Central Siberia. 1—location of the study area, 2—location of the sampling site, 3–6—boundaries of modern geographical ranges of tree species [40]: 3—*Pinus sylvestris*, 4—*Abies sibirica*, 5—*Pinus sibirica*, 6—*Picea obovata*.

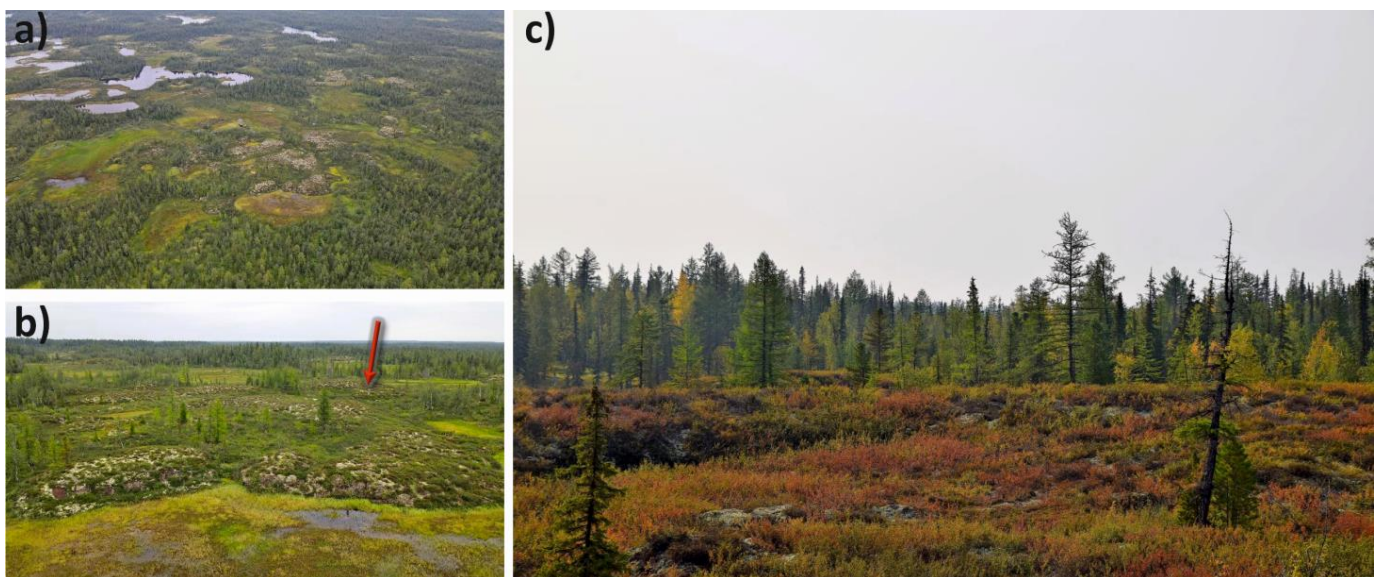


Figure 2. Views of the peatland and its forest environment: (a). The Igarka peatland, top view; (b). the Igarka peatland and perennial frost mounds, the red arrow indicates the core sampling site; (c). forest surrounding the peatland.

The Igarka peatland covers an area of 12.4 ha and consists of ridges of perennial frost mounds (palsas) up to 5 m high and over 100 m wide, separated by thawed hollows (200–300 m). The plant cover of the palsa consists of lichens (70%) and feathermosses (20%) with *Betula nana* L. and *Ledum palustre* L. The vegetation of the hollows is formed by various species of *Carex*, feathermosses and *Betula nana* thickets [38].

2.2. Sediment Sampling and Radiocarbon Dating

The 860 cm long sediment core recovered from the perennial frost mound (4.5 m high and about 100 m wide) was used to obtain the high-resolution pollen and macrocharcoal records. A portable drilling station equipped with a motorized piston corer was used to collect the core in late August 2020.

The sediment core comprised peat deposits (845 cm) with numerous ice lenses and a layer of unstratified dark gray clay with plant detritus (15 cm). The lower part of the peat sequences (845–516 cm) is formed by highly humified minerotrophic peat composed of the remains of feathermosses such as *Hamatocaulis vernicosus* (Mitt.) Hedenäss, *Drepanocladus aduncus* (Hedw.) Warnst., and *Scorpidium scorpioides* (Hedw.) Limpr. [38]. Alternation low-decomposed peat horizons with dominance of *Sphagnum* mosses (*Sphagnum girgensohnii* Russow, *S. teres* (Schimp.) Ångstr., and *Sphagnum squarrosum* Crome) and highly decomposed peat with remains of feathermosses, herbs, and *Carex* occur between 516 and 220 cm. *Carex* species (*C. chordorrhiza* Ehrh., *C. lasiocarpa* Ehrh., and *C. aquatilis* Wahlenb.) predominate among the peat-forming plants, which alternate with the layers of brown and feathermosses in the depth interval 220–51 cm and are replaced by peat with *Eriophorum vaginatum* L., *Scheuchzeria palustris* L., and abundant *Sphagnum* stems between 51 and 17 cm. The uppermost layer of the peat sequence is represented by remains of *Ledum palustre*, *Cladonia*, *Cetraria*, and *Polytrichum strictum* Brid.

Pollen was sampled at 5 cm intervals. Macrocharcoal samples were collected continuously, with sampling intervals varying from 0.5 to 5.0 cm (average 2.8 cm) depending on the amount of ice and peat material in the samples. In total, 136 pollen samples and 537 macro-charcoal samples were analyzed.

The radiocarbon dating was performed for 20 bulk peat samples (Table 1). The samples were first prepared at the Center of Common Use “Laboratory of Radiocarbon Dating and Electronic Microscopy” of the Institute of Geography of the Russian Academy of Sciences (Moscow), and then dated by accelerator mass spectrometry at the Center for Applied Isotope Studies of the University of Georgia (USA). The “Bacon” package [41] in the R language environment [42] was used to calculate the age–depth model (Figure 3). Calibration of ^{14}C dates was performed with the “Bacon” package using the Intcal 20 calibration curve [43].

Table 1. Radiocarbon dating of the peat from the Igarka peatland.

Laboratory Code IGAN _{AMS}	Depth, cm	Material	^{14}C yr. BP, 1σ	Age, cal. yr. BP, 2σ (Probability)
8354	15	TOC ¹	1930 ± 20	1817–1896 (0.806)
8332	50	TOC	3230 ± 20	3391–3468 (0.965)
8333	60	TOC	3320 ± 20	3480–3574 (0.987)
8334	101	TOC	3430 ± 20	3617–3723 (0.820)
8335	150	TOC	3805 ± 20	4144–4248 (0.874)
8336	202	TOC	4120 ± 20	4528–4654 (0.545)
8337	252	TOC	4080 ± 20	4518–4624 (0.793)
8338	301	TOC	4320 ± 20	4840–4888 (0.797)
8339	351	TOC	4360 ± 20	4857–4973 (1.000)
8340	402	TOC	4445 ± 20	4962–5070 (0.549)
8341	449	TOC	4340 ± 20	4851–4960 (1.000)
8342	500	TOC	4490 ± 20	5155–5288 (0.569)
8343	550	TOC	4830 ± 20	5574–5596 (0.582)
8344	599	TOC	4955 ± 25	5601–5729 (1.000)
8345	650	TOC	4315 ± 25	4837–4888 (0.772)

Table 1. Cont.

Laboratory Code IGAN _{AMS}	Depth, cm	Material	¹⁴ C yr. BP, 1σ	Age, cal. yr. BP, 2σ (Probability)
8346	700	TOC	5165 ± 20	5900–5942 (0.827)
8347	749	TOC	5200 ± 20	5916–5994 (1.000)
8348	798	TOC	5400 ± 20	6187–6282 (0.954)
8349	845	TOC	5425 ± 20	6198–6287 (1.000)
8350	860	TOC	5500 ± 20	6276–6315 (0.898)

¹ TOC—total organic carbon.

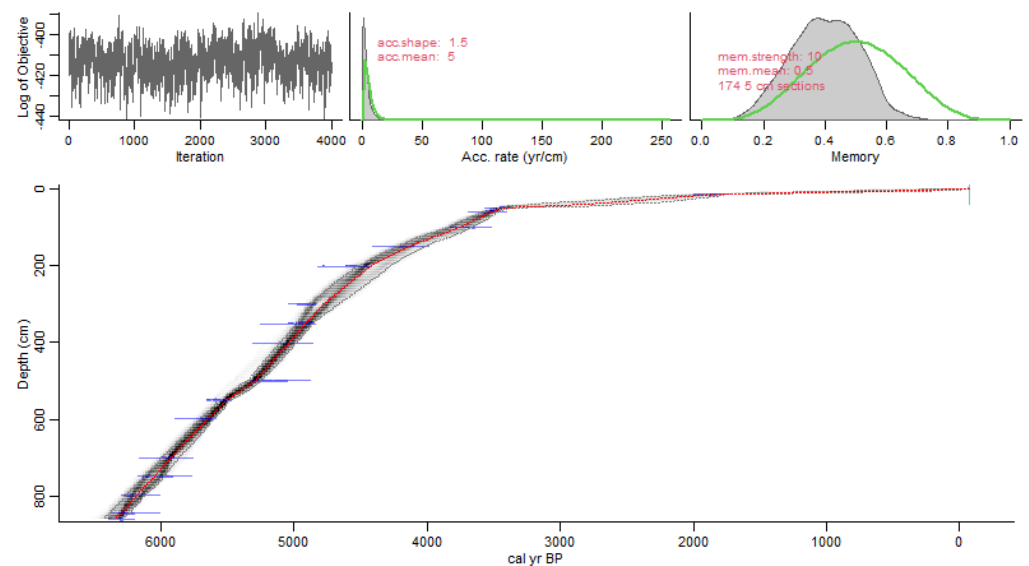


Figure 3. Bacon R script age-depth model (red dotted line), random walks (grayscale), and 95% CI (dotted gray lines) of twenty radiocarbon dates (distributions in blue) and parameter settings (red text at top right) for the peat core from the Igarka peatland (modified after Novenko et al. [38]).

2.3. Pollen Analysis

Peat samples for pollen analysis (1 cm³) were prepared according to Moore et al. [44]. The samples were heated in 10% KOH for 10 min to remove humic material. The residue was then sieved through a 200 µm mesh, followed by HF treatment [45]. The residue was then finely sieved through 10 µm mesh with 10% Na₄P₂O₇ in an ultrasonic bath for less than one minute. The sample preparation was completed by acetolysis in a water bath for 5 min, using propionic anhydride [46] to dissolve the cellulose. *Lycopodium* spores were added prior to chemical treatment to determine pollen and charcoal concentrations [47]. Pollen identification was performed using a Zeiss Axio Lab A1 microscope at 400× magnification according to Reille [48] and Beug [49]. Identification of non-pollen palynomorphs (NPPs) is based on van Geel [50], Shumilovskikh et al. [51], and the NPP Image Database [52]. The calculation of pollen percentages was based on the total terrestrial pollen sum, i.e., arboreal pollen (AP) plus non-arboreal pollen (NAP), excluding aquatic plants, spores, and NPPs. At a minimum, 350–400 pollen grains were counted per sample (AP + NAP). Microscopic charcoal (<100 µm) concentrations were assessed using Clark’s point-count method [53]. Pollen and plant macrofossil diagrams were created using the programs Tilia and TGView [54].

During the extraction of the peat core in the field, four large wood fragments (up to 5 cm in length) were found and identified according to Benkova and Schweingruber [55].

2.4. Charcoal Analysis

Macroscopic charcoal analysis was used to determine the frequency of forest fires. Samples of fresh peat with volume of 1 cm³ were stored in bleach (100 mL of 10% NaOCl) at room temperature for 24 h [56]. Then, the samples were gently sieved through a 125 µm mesh and the residue was carefully placed on labelled Petri dishes and charcoal particles were registered using the MOTIC SMZ-171 stereoscopic microscope at 40× magnification. Data processing for charcoal analysis was performed in the “Tapas” package version v.0.1.0 [57] in the R language environment [42]. In our study, we used the following parameters: charcoal concentration (pieces cm⁻³), charcoal accumulation rate (pieces cm⁻² yr⁻¹, CHAR), CHAR of the interpolated record (C_{int}), and the low-frequency trend in CHAR (C_{back}). We used a 10-year period to interpolate the record, which allows accurate documentation of peaks at relatively high peat accumulation rates. The peaks of the charcoal accumulation were determined as a relationship: C_{peak} = C_{int} - C_{back} [57]. We assume that the peaks of the charcoal accumulation rate indicate the local fire episodes (one or several successive fires). These peaks were separated from the background charcoal (C_{back}) using the method of smoothing time-series data using moving medians. A 300-year window was used to smooth the data set for C_{back} estimation. The corresponding threshold value within the C_{peak} component was set at the 95th percentile of the Gaussian mixture model.

2.5. Climate Reconstruction

The best modern analogue (BMA) technique was used to reconstruct the mean July temperature and annual precipitation. Details of the BMA approach are presented in many publications devoted to paleoclimate research [58–62] and references therein. Using the BMA technique, we compare the fossil pollen assemblage with modern pollen assemblages. We use squared-chord distances (SCD) [58] as an index of dissimilarity. In the present study, we consider two spectra to be analogous if their SCDs were less than the threshold equal to 2. The reconstructed values of temperature and precipitation were calculated as weighted averages of 8 modern analogues. The BMA calculations were performed in the “analogue” package [63] in the R language environment [42] (see Supplementary Material S1).

The training set of the modern pollen assemblages in our study includes 173 pollen spectra from different landscapes in the northern Siberia and Yakutia. A total of 142 sites were derived from the Eurasian Modern Pollen Database-2 [64], and 30 pollen assemblages are our own surface samples collected in the period 2020–2022 in the area of Igarka and several regions of Central Siberia. Climatic information was obtained from the reference book “Climate of Russia” [36].

Leave-one-out cross-validation [65] showed a relatively good correlation of the pollen-based July temperature and annual precipitation reconstructions with modern climate characteristics. We obtained R-squared (R² = 0.89, *p* < 0.05), root mean squared error (RMSE = 1.2 °C), and mean absolute error (MAE = 0.77 °C) for the mean July temperature and R² = 0.79, RMSE = 51 mm, and MAE = 32 mm for the mean annual precipitation, which is basically sufficient for reconstructing climate changes during the Holocene.

3. Results

3.1. Chronology

According to the data obtained, the accumulation of the sediment core began at 6320 cal yr BP. With a sampling interval of 50 cm, the radiocarbon dates show a progressive increase in age downwards (Figure 3, Table 1), except for a few inversions. The ¹⁴C dates at the depths of 252 cm (¹⁴C 4080 ± 20 yr BP) and 449 cm (¹⁴C 4340 ± 20 yr BP) revealed the ages lying within the uncertainty of the model of the linear peat growth (Figure 3). A sample from the depth of 650 cm (¹⁴C 4315 ± 25 yr BP) indicated a much younger age as compared to the over- and under-lying samples, probably due to the bioturbation or sampling error.

The age of most of the peat core corresponds to the time interval between 5500 ± 20 ¹⁴C yr BP (6320 ± 20 cal yr BP) and 3230 ± 20 ¹⁴C yr BP (3440 ± 20 cal yr BP), as indicated by

radiocarbon dates derived from depths of 860 cm and 50 cm, respectively. Thus, the average temporal resolution of the peat core, except for the uppermost 50 cm, varies from 0.25 to 7 yr cm⁻¹. This rate of peat accumulation is extraordinarily high compared to the average peat growth in Western Siberia [66,67] and could be overestimated due to peat expansion by ground ice lenses in the perennial frost mound. We observed several ice layers up to 5 cm thick in the studied peat core, as well as numerous inclusions of ice crystals in the peat. Nevertheless, the specificity of peat growth in the period 6320–3440 cal yr BP gives us the opportunity to perform the paleoenvironmental reconstruction with decadal resolution.

The peat accumulation rate decreased significantly between 3440 and 1850 cal yr BP, as indicated by the radiocarbon date of 1930 ± 20 ¹⁴C yr BP (1850 ± 40 cal yr BP) found at a depth of 15 cm. The average temporal resolution of this peat layer is about 42 yr cm⁻¹. The chronology of the uppermost 15 cm of the peat core above the ¹⁴C date 1930 ± 20 yr BP is unclear. We suggest that the peat accumulation rate may be underestimated because of peat disturbances in the result of water erosion of the palsa surface and wildfires. During the field observations, we recorded patches of bare peat and cracks on the palsa surface and slopes and found charcoal fragments and charred wood at the depths of 10–11 and 13–14 cm. The damage of the uppermost peat layers in perennial frost mounds and peat plateaus is common for peatlands in the Arctic region [32,67].

3.2. Pollen Analysis and Vegetation History

The results of pollen analysis showed that the vegetation dynamics over the past 6320 years was an alternation of phases of middle-taiga forests of *Larix*, *Pinus sibirica*, *Picea*, and *Abies* (intervals 6320–6050, 5790–5370, 4480–4220, and 3600–2700 cal yr BP, respectively) and open *Larix* woodlands with the participation of *Picea*, *Pinus sibirica*, and *Betula*, typical for northern-taiga (intervals 5370–4480, 4220–3600 cal yr BP and 2760 cal yr BP–present, respectively). Eight pollen assemblage zones (PAZ) were identified in the pollen diagram of the studied peat core (Figure 4).

PAZ 1 (865–750 cm, 6320–6050 cal yr BP). Arboreal pollen predominated in the assemblages (90%–98%), mainly due to the high pollen values of *Pinus*, *Betula alba*-type (40%–70%), and shrubs (*Betula nana*, *Alnus fruticosa* Rupr.). The proportion of *Picea* and *Abies* pollen did not exceed 10%–20%. Pollen of *Juniperus* and *Salix* occurred in small quantities. Non-arboreal pollen was represented by Poaceae, Cyperaceae, *Artemisia*, and Rosaceae (0.5%–2%). With slight variations in abundance, these taxa were consistently recorded throughout the peat sequence. Pollen of Onagaraceae occurred sporadically. The group of spores was abundant and diverse. Spores of *Lycopodium annotinum* L. (up to 40%), *L. clavatum* L., *L. pungens* (Desv.) Bach. Pyl. ex Iljin, and Polypodiaceae (up to 10%) were recorded; values of *Equisetum* reached 70%–100% compared to the sum of AP + NAP. Aquatic plants included pollen of Nymphaeaceae, *Alisma*, and *Menyanthes trifoliata* L. The high concentration of microscopic charcoal particles was revealed. *Gelasinospora* was also found.

PAZ 2 (750–650 cm, 6050–5790 cal yr BP). Although arboreal pollen values remained high (85%–85%), tree pollen noticeably declined (to 40%) while shrubs become more abundant. Pollen values of dwarf birch (*Betula nana*) increased from 5%–7% to 40%–50%. The share of *Picea* and *Abies* dropped to a few percent, and the *Pinus* pollen value decreased to 20%–30%. The composition of herbaceous pollen and spores was similar to the previous zone, except for a lower proportion of *Lycopodium annotinum* (2%–3%). *Menyanthes trifoliata* and *Typha latifolia* L. were identified among the wetland plants. The concentration of microscopic charcoal particles reached its maximum value throughout the peat core. *Gelasinospora* was found in several samples.

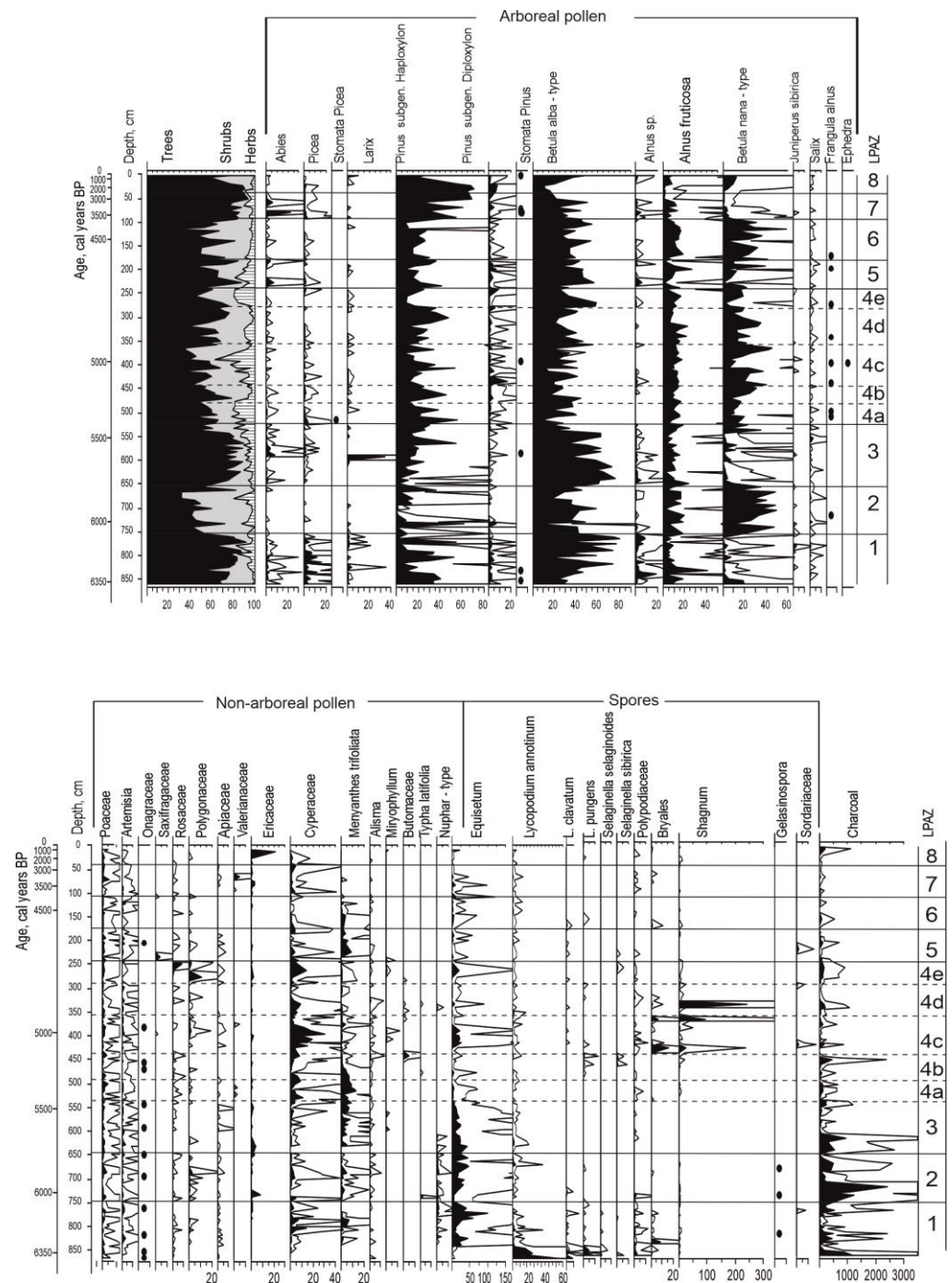


Figure 4. Percentage pollen diagram of the Igarka peatland. Pollen sum: AP + NAP; additional curves represent $\times 10$ exaggeration of base curves; black dots indicate the presence of taxa $<1\%$.

PAZ 3 (650–520 cm, 5790–5370 cal yr BP). The composition of pollen assemblages in this zone was similar to PAZ 1. Tree pollen values increased to 80%–90%, mainly due to pollen of *Betula alba*-type. The pollen curves of *Picea*, *Abies*, and *Larix* formed noticeable peaks. The proportion of *Betula nana* reduced to 5%–10%. The concentration of microscopic charcoal gradually declined.

PAZ 4 (520–225 cm, 5370–4480 cal yr BP). Pollen assemblages are characterized by a decrease in AP to 60%–80%, and tree pollen values decreased to 40%–50%, with the exception of *Pinus*. At the same time, the proportion of shrubs grown as *Betula nana* and *Alnus fruticosa* increased to 30%–50% and 10%–15%, respectively. Pollen values of *Pinus* subgen. *Haploxyton* varied from 40% to 60%, and *Pinus* subgen. *Diploxyton* reached 5%–7%. Cyper-

aceae and *Menyanthes trifoliata* dominated the NAP. Pollen grains of *Ephedra* were found. *Equisetum*, *Sphagnum*, and bryales are common among the spores. *Selaginella selaginoides* (L.) Link appeared.

Fluctuations in the AP/NAP ratio and several peaks in the spore group allowed us to divide this zone into 5 subzones. Subzones 5a (520–420 cm), 5c (420–350 cm), and 5e (270–225 cm) were characterized by a decrease in tree pollen value (to 80% in subzone 5a and 5e and up to 60% in subzone 5c) and an increasing proportion of Cyperaceae, *Menyanthes trifoliata* (subzone 5a), *Equisetum*, and Polypodiaceae (subzone 4c). Arboreal pollen content increased to 90%–95% in subzone 5b (450–420 cm) and 5d (350–270 cm), mainly due to pine pollen. High peaks (200%–300% of AP + NAP) of *Sphagnum* mosses were detected.

PAZ 5 (225–170 cm, 4480–4220 cal yr BP). The proportion of arboreal pollen grew, *Picea* and *Abies* formed several peaks up to 10%, and the share of *Betula alba* pollen increased up to 50%. Cyperaceae, Saxifragaceae, and *Menyanthes trifoliata* were abundant in the NAP. Charcoal content was low.

PAZ 6 (170–90 cm, 4220–3600 cal yr BP). The pollen assemblages revealed the opposite tendency of the decline of tree pollen value (up to 40%–50%) and increase in *Betula nana* (30%–50%) and *Alnus fruticosa* (15%–25%). *Picea*, *Abies*, and *Larix* decreased significantly, while *Pinus* (20%–30%) and *Betula* (40%–50%) maintained their high proportions. NAP was scanty. Spores were represented by *Equisetum* (3%–5%) and single spores of *Sphagnum* and *Lycopodium annotinum*, *L. clavatum*.

PAZ 7 (90–45 cm, 3600–2700 cal yr BP). The pollen assemblage was characterized by the largest proportion of *Abies* (20%–25%) and high pollen values of *Picea* (10%–12%) and *Pinus* subgen. *Haploxylon* (45%–50%). Shrubs were significantly reduced (10%–12%) and represented mainly by *Alnus fruticosa*. The proportion of NAP and spores (mainly Poaceae, Cyperaceae, *Artemisia*, *Valeriana*, Polypodiaceae, and *Equisetum*) did not exceed 5%–7%.

PAZ 8 (45–0 cm, 2760 cal yr BP–present) corresponds to the uppermost layer of highly humified peat. Pollen concentration in these samples was extremely low, and pollen preservation was poor. Pollen assemblages were dominated by *Pinus*, *Betula*, shrubs, and Ericaceae. Microscopic charcoal concentration increased at the depths of 10–15 cm.

The wood fragments found during the extraction of the peat core were identified as two remains of *Larix* sp. (samples from depths of 825.5–830.5 cm and 832–834 cm) and two remains of *Alnus fruticosa*, obtained at depths of 846–847 cm and 859–860 cm.

3.3. Macroscopic Charcoal and Fire History

The reconstruction of the fire history from the macro-charcoal data is based on the hypothesis that most of the charcoal particles with a size > 125 μm were deposited between a few meters and 1–3 km away from the fire [57,68]. Long-range transport (from a distance of more than 3 km away) of macroscopic charcoal is an unlikely pathway for the particles to reach the sample plots.

Macro-charcoal concentration is high (180–670 particles cm^{-3}) in the lower part of the peat core (851–836 cm). The highest peak of macro-charcoal concentration (up to 860 pieces cm^{-3} , Figure 5) was detected in the lowest peat layer at the depth of 847 cm. Except for this part of the peat core, the macro-charcoal concentration did not exceed 1–10 pieces cm^{-3} , and at several depths no charcoal particles were found.

Macro-charcoal analysis of the peat core revealed the highest CHAR value between 6200 and 5600 cal yr BP, C_{int} ranged from 100 to 140 pieces $\text{cm}^{-2} \text{yr}^{-1}$ with a peak of up to 290 pieces $\text{cm}^{-2} \text{yr}^{-1}$ at 6300 cal yr BP, and C_{back} varied in the interval 1–15 pieces $\text{cm}^{-2} \text{yr}^{-1}$ (Figure 4). Thirteen fire episodes were identified, with fire return intervals (FRI) ranging from 10 to 120 years.

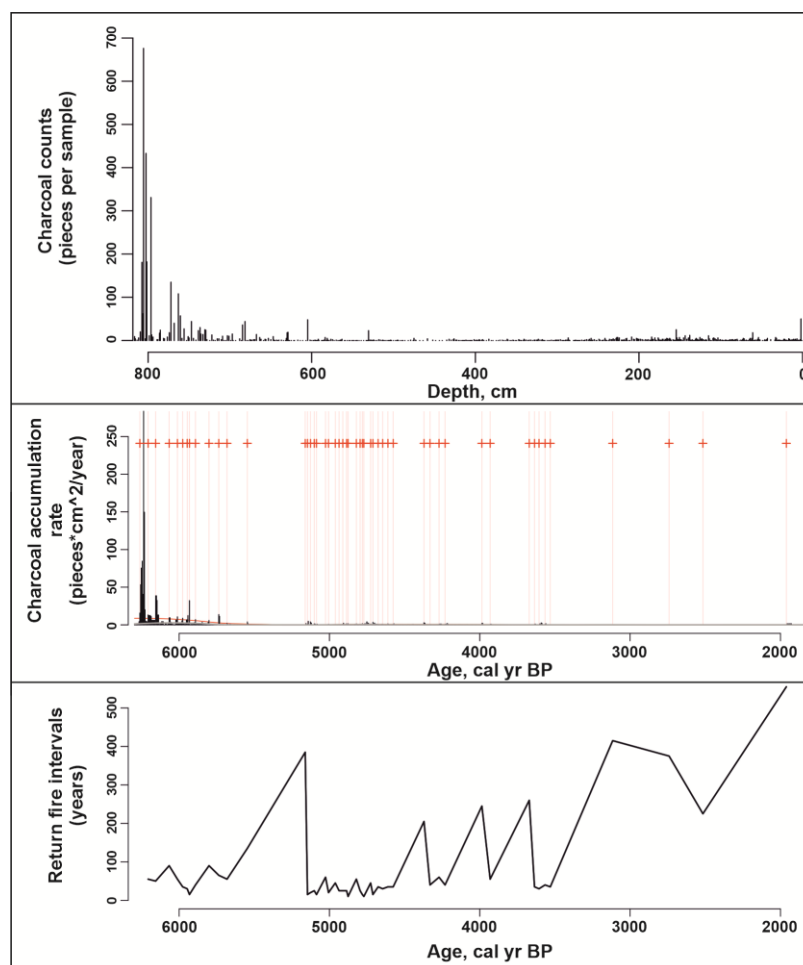


Figure 5. Temporal variability of macroscopic charcoal concentration, charcoal accumulation rate in the Igarka peatland, and fire return interval. Red + indicates fire episodes.

After 5600 cal yr BP, the accumulation of macroscopic charcoal decreased by an order of magnitude, and C_{int} did not exceed $10 \text{ pieces cm}^{-2} \text{ yr}^{-1}$ until the present. During the period 5600–4800 cal yr BP, C_{int} varied from 0 to 5 $\text{pieces cm}^{-2} \text{ yr}^{-1}$, C_{back} was below $0.4 \text{ pieces cm}^{-2} \text{ yr}^{-1}$, no fire episodes were identified, and FRI increased to 750 years.

A slight increase in CHAR value was observed between 4700 and 3900 cal yr BP, and C_{int} ranged between 0.5 and 7 $\text{pieces cm}^{-2} \text{ yr}^{-1}$. Fifteen fire episodes were identified with FRI 10–90 years. However, the low CHAR values suggest a series of low-intensity fires in the area close to the peatland. During the time interval 3900–3650 cal yr BP, the charcoal accumulation in the peatland ceased, FRI was 250 years. Between 3650 and 3550 cal yr BP, there was a short-term increase in charcoal accumulation. C_{int} increased to 5–7 $\text{pieces cm}^{-2} \text{ yr}^{-1}$, and C_{back} was about 7 $\text{pieces cm}^{-2} \text{ yr}^{-1}$ with FRI 20–25 years. After 3550 cal yr BP, charcoal input declined to insignificant values. FRI expanded to 1600 years.

4. Discussion

The results, based on the analysis of pollen and macro-charcoal from the Igarka peatland, allowed us to discuss the changes in vegetation and the history of fires in the northern Yenisei Siberia during the middle- and late-Holocene (Figure 6). Peat inception in the Igarka peatland occurred around 6320 cal yr BP during the Holocene thermal maximum. An abundance of *Larix* sp. and *Alnus fruticosa* macroremains in plant macrofossil assemblages [38] and the finding of fragments of their wood in the basal horizon of the peat sequence suggest paludification of the wet larch forest and further development of the peatland.

The Igarka pollen record showed an expansion of middle-taiga forests of *Larix*, *Pinus sibirica*, *Picea*, and *Abies* between 6320 and 5360 cal yr BP. The proportion of *Larix* in the pollen assemblages varied from 0.1% to 4.5%, except for a peak of up to 30% at a depth of 590 cm. According to studies on the pollen productivity of the main Arctic species [69] and the composition of surface pollen spectra from larch forests in different regions [70–72], *Larix* is strongly underestimated in pollen spectra as compared to its abundance in the vegetation. The percentage of *Larix* pollen in Northern Siberia rarely exceeds 3%–5% [70,73]. Relatively high pollen values of *Abies* and *Picea* indicated the tendency of climate warming and northward shift of vegetation-zone boundaries. The northern limit of the geographical range of *Abies sibirica* lies about 200 km south of the study area (Figure 1, [40]), and the abundance of its pollen likely indicates warmer climatic conditions. Warmer-than-present climatic conditions during the Holocene thermal maximum are suggested by the frequent occurrence of *Nymphaea* pollen in the assemblages. Species of *Nymphaea* need higher summer temperatures for growth and flowering in Siberia compared to the modern temperature conditions in the Igarka area [74].

Reconstructions of the mean July temperature in Igarka for the period 6320–5360 cal yr BP using the BMA approach showed a high variability of temperatures in the range of 14.7 to 17.3 °C with several abrupt minima (Figure 6). However, most of the values obtained showed positive temperature anomalies with respect to modern values. The reconstruction of June–July temperature on the Yamal Peninsula by dendrochronological data [75] showed an increase in summer temperatures up to 13.5 °C around 6300 cal yr BP and a progressive cooling after 5800 cal yr BP. Our results are in good agreement with the pollen-based temperature reconstructions from several lakes in the Russian Arctic, such as Lama Lake in the northwest of the Putorana Plateau [13], Levinson-Lessing Lake [12,14], and the lake around Khatanga [76] in the northern Taimyr Peninsula, that indicate a warm climate and several positive July temperature anomalies in the period between 7000 and 5000 cal yr BP. Chironomid-based temperature reconstructions, and diatom and stable isotope records from lake deposits in Yakutia [19,20,77] revealed a remarkable climate warming between ca. 6000 and 4500 cal yr BP.

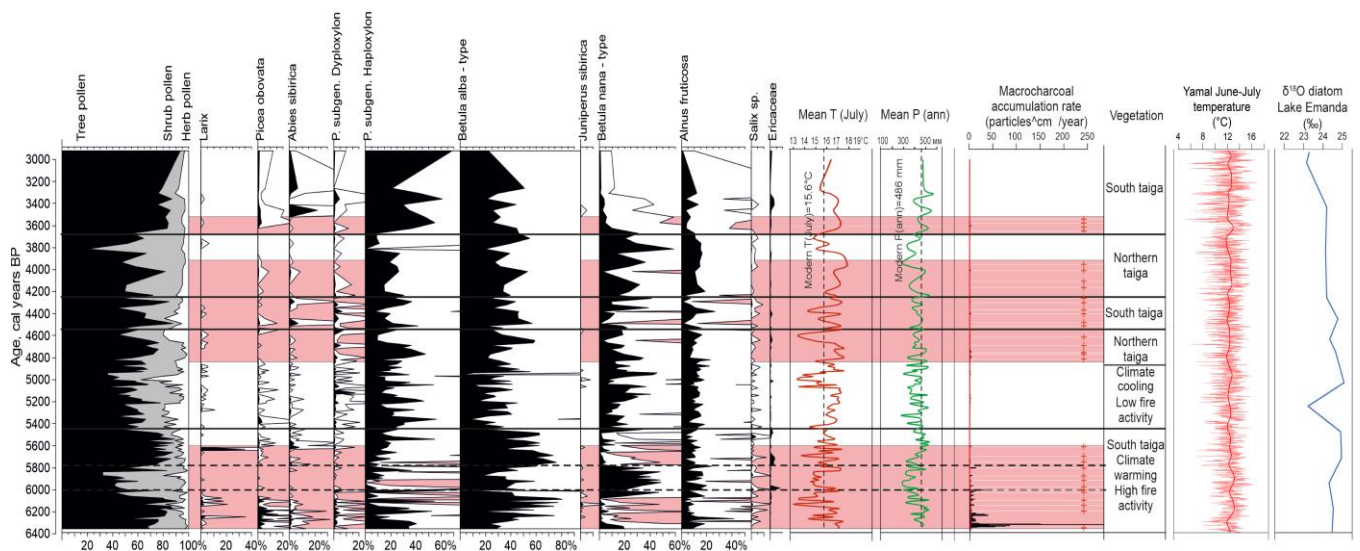


Figure 6. Results of the multi-proxy analysis of the Igarka peatland, including characteristic pollen taxa, macrocharcoal accumulation rate with fire episodes, reconstructions of the mean July temperature and the mean annual precipitation compared to the Yamal June–July temperature inferred from dendrochronological data [75], and the oxygen isotope composition of diatoms from Lake Emندا (Yakutia) [77]. Pink bands indicate periods of high fire frequency.

The period between 6320 and 5790 cal yr BP was characterized by a high level of fire activity and an intensive accumulation of charcoal in the peat. The high concentration of micro- and macroscopic charcoal in the interval 6320–6000 cal yr BP, two orders of magnitude higher than its average content in the peat core, as well as the finding of charred plant remains and charcoal fragments by plant macrofossil analysis [38], suggest a fire adjacent to the peatland. The fire return interval ranged from 70 to 120 years and was significantly shorter than the modern interval inferred for the northern-taiga region of Central Siberia from fire scars on larch trunks [78]. The pollen record revealed a phase of abrupt decrease in tree pollen values and high abundance of *Betula nana* between 6050 and 5790 cal yr BP (Figure 6). Changes in pollen assemblages were more likely caused by post-fire succession of plant cover rather than vegetation dynamics caused by climatic variability. The occurrence of spores of the mainly carbonaceous fungus *Gelasinospora* sp. provided additional independent evidence that fires had occurred in the peatland [50,51]. We suggest that frequent forest fires without human influence may have been caused by climatic conditions, such as summer droughts. Reconstruction of mean annual precipitation using pollen data from the Igraka peatland (Figure 6) revealed a decrease in climatic wetness in 6200–5600 cal yr BP, which could contribute to higher fire frequency. A study of fire history in Northern Siberia [24,26] showed high charcoal accumulation in the mid-Holocene, which also coincides with the high charcoal accumulation rates recorded in the Lake Baikal region [27].

According to the pollen data from the Igraka peatland, the forest canopy was gradually reduced from 5360 cal yr BP; the middle-taiga vegetation was replaced by larch woodlands with spruce, pine, and some herbaceous plants that are typical for the northern taiga (Figure 6). *Pinus sibirica* dominates the pollen assemblages between 5360 and 4465 cal. years BP, and pollen of *Pinus sylvestris* is also found in small amounts (up to 5%–10%), although it is currently growing about 300 km to the south of the study area (Figure 1 in [40]). Studies of surface pollen assemblages in Northern Siberia [70,73] have shown that in sparse or open-plant communities, i.e., where the proportion of pollen transported by the wind is higher, the maximum values of both pine species are reached.

Reconstructions of July temperature at Igarka revealed three intervals of significant climate cooling in 5400–5480, 5075–4940, and 4670–4550 cal yr BP, when the temperature of the warmest month decreased to 13.5–13.7 °C. Our findings are consistent with the estimation of Yamal summer temperatures inferred from tree-ring chronologies [75], the oxygen isotope composition of diatoms from Lake Emanda [76] (Figure 6), and pollen-based climate reconstructions from Lama Lake [13] and a lake around Khatanga [75], which show a climatic deterioration after 5200–5000 cal yr BP. Paleoclimatic studies based on various proxies in Northern Eurasia show a noticeable cooling and glacial advance in mountainous areas after 5500 cal yr BP [79], apparently caused by a decrease in summer solar radiation [80].

The low recovery of macro- and micro-charcoal remains in the peat core from the Igarka mire (Figure 5) suggested a decline of fire activity in the study area, which could be an indirect sign of a humid summer. However, reconstruction of the mean annual precipitation in Igarka using the BMA technique showed relatively low values, ranging from 350 to 500 mm per year. We suggest that during the cooler and possibly shorter summers, evaporation was reduced, which could lead to an increase in soil moisture in many habitats [81], creating unfavorable conditions for the occurrence and spread of forest fires [82].

During the time interval between 4465 and 2700 cal yr BP, three phases of vegetation changes have been identified. A higher proportion of woody vegetation in the plant cover, expansion of *Abies*, and the increase in *Picea* abundance in forest stands occurred in 4465–4200 and 3600–2700 cal yr BP, indicating climate warming and a shift northward of the boundary between the middle- and northern-taiga. Biomass burning increased and FRI became shorter, but the low value of charcoal input (Figures 5 and 6) suggests low-intensity fires in the area adjacent to the Igarka peatland. Frequent fires may promote

local permafrost thawing, creating better conditions for tree growth and regeneration [83], and likely favoring the expansion of spruce and fir species. The reduction of the forest canopy and the expansion of birch and shrubs (*Alnus fruticosa*, *Betula nana*), apparently caused by climate cooling, were detected in 4200–3600 cal yr BP.

Reconstructions of the July temperature at Igarka show a number of positive and negative anomalies for summer temperatures, most of which agree well with pollen data, but, in some intervals, the reconstructed summer temperature contradicts vegetation changes inferred from pollen records. Inconsistencies between pollen and climate reconstructions can be explained by the weaknesses of the BMA approach in the situation of limited modern pollen assemblages [62]. Nevertheless, the phase of southern-taiga corresponded to the increase in July temperature to 16.9–17.2 °C between 3620–3300 cal yr BP and the phase of the remarkable reduction of forest canopy in 3860–3670 cal yr BP corresponded to the climate cooling and the temperature drop to 14.9 °C. Our results are largely in agreement with chironomid-based July temperature reconstructions from two mountain lakes in the western part of the Putorana Plateau [84], which suggest a warmer climate between 3900 and 3400 cal yr BP than at present and a subsequent cooling with the maximum at 2500 cal yr BP. Paleoclimatic records based on pollen from Lama and Levinson-Lessing lakes [13,14] showed several positive temperature anomalies for July between 4700 and 3600 cal yr BP. Reconstruction of Yamal June–July temperatures from tree-ring records revealed a high variability of summer conditions with a pronounced mid-to-late Holocene cooling trend [75].

After 2700 cal yr BP, the vegetation cover of the study area becomes very similar to the modern pattern. Pollen assemblages show a gradual decrease in *Picea*, *Abies*, and *Larix* pollen values, while the proportion of pine, dwarf birch, and shrubs increases, indicating an expansion of northern-taiga woodlands. However, since the uppermost part of the peat sequences was obviously partly destroyed by water erosion and forest fires, and the sampling resolution for the last 2700 years was low, the chronology for the last ca. 1800 years is unclear, which did not allow us to reconstruct vegetation changes in detail.

Climate change since ca. 2700 cal yr BP was evidenced by numerous proxy data from Siberian Arctic regions [12,75–77,83–85], Yakutia [76], and data from a global scale [86]. The clearly manifested cooling trend was revealed from dendroclimatological reconstruction and analysis of the frequency of abnormal anatomical structures in the larch and spruce wood from the Yamal peninsula [87]. Time-coeval pollen data from the peatland at Igarka near the study site [39] indicated the degradation of the dark coniferous taiga and the expansion of sparse larch-birch woodlands and shrub communities formed mainly by *Betula nana* and *Alnus fruticosa*. Pollen records from the more northerly coastal regions of the Taymyr Peninsula [13] and even further to the northeast, including the coastal regions of the Eastern Arctic seas [88] also testify to the stabilization of vegetation-zone boundaries around 2500 cal yr BP. Further vegetation changes were apparently caused by local peat development processes, wildfires, and human impact.

5. Conclusions

The new high-resolution pollen and charcoal data from the perennial frost mound in the peatland near the town of Igarka provide a unique opportunity to investigate the mid- to-late Holocene forest and fire history in this very remote and poorly documented area of Yenisei Siberia. Our findings suggest several phases of vegetation change between 6320 and 2700 cal yr BP, influenced by climatic fluctuations and fire occurrence. During the Holocene thermal maximum and the periods of warming (6320–5360, 4465–4200, and 3600–2700 cal yr BP), the eastern margin of the West Siberian Lowland was occupied by middle-taiga larch forests with a high proportion of *Abies sibirica*, *Picea obovata*, and *Pinus sibirica*. Climate warming caused a northward shift of the vegetation-zone boundaries in the Yenisei Siberia. The area of distribution of *Abies sibirica* expanded by 200 km northward compared to its modern range. Fire frequencies and biomass burning increased during the warming periods. We suggest that the frequent fires may encourage the melting of the

local permafrost, thereby enhancing tree growth and regeneration, and likely favoring the expansion of *Abies sibirica* and *Picea obovata* farther to the north.

Climate deterioration at 5400–5480, 5075–4940, 4670–4550, and 3860–3670 cal yr BP led to a degradation of the dark coniferous forests in the study area. This was caused by the expansion of sparse larch-birch woodlands with an admixture of *Picea obovata* and *Pinus sibirica* and shrub communities dominated by *Betula nana* and *Alnus fruticosa*. The cooling of the climate was accompanied by a decrease in the frequency of fires.

Although the uppermost part of the studied peat sequences was partly destroyed by water erosion and wildfires and the sampling resolution was low, we assume that the vegetation pattern of the region became close to the modern one at around 2700 cal. yr BP. Based on the comparison of modern environmental processes with periods of climate warming and increased fire activity in the past, we suggest a potential increase in suitable habitats for tree growth in Yenisei Siberia in the future, and further studies are needed to test this hypothesis.

Supplementary Materials: The following supporting information can be downloaded at: <https://www.mdpi.com/article/10.3390/f14122321/s1>, S1. R Code for the modern analogue technique.

Author Contributions: Investigation, E.N., O.R., N.M., D.K., R.A., A.S., M.K. and A.P.; data curation, R.A., D.K. and A.P.; writing—original draft preparation, E.N.; writing—review and editing, E.N. and A.O. All authors have read and agreed to the published version of the manuscript.

Funding: Field works: radiocarbon dating, charcoal, and pollen analysis were supported by the Russian Science Foundation (grant number 20-17-00043). Reconstructions of climate changes and fire history were supported by the State assignment FMGE-2019-0005. Data analysis and paper preparation were funded by Megagrant project (agreement 075-15-2021-599, 8 June 2021). The analysis of climate anomaly—fire frequency interaction conducted by A. Olchev was supported by the Russian Science Foundation (grant number 22-17-00073).

Data Availability Statement: The data presented in this study are available on request from the corresponding author.

Acknowledgments: The authors are very grateful to colleagues from Igarka Geocryological Laboratory and Melnikov Institute of Permafrost SB RAS for appreciable help in field work.

Conflicts of Interest: The authors declare no conflict of interest.

References

1. IPCC. *Climate Change 2022: Impacts, Adaptation, and Vulnerability*; Contribution of Working Group II to the Sixth Assessment Report of the Intergovernmental Panel on Climate Change; Pörtner, H.-O., Roberts, D.C., Tignor, M., Poloczanska, E.S., Mintenbeck, K., Alegría, A., Craig, M., Langsdorf, S., Lösschke, S., Möller, V., et al., Eds.; Cambridge University Press: Cambridge, UK; New York, NY, USA, 2022; 3056p. [\[CrossRef\]](#)
2. Callaghan, T.V.; Björn, L.O.; Chernov, Y.; Chapin, T.; Christensen, T.R.; Huntley, B.; Ims, R.A.; Johansson, M.; Jolly, D.; Jonasson, S.; et al. Biodiversity, Distributions and Adaptations of Arctic Species in the Context of Environmental Change. *AMBIO* **2004**, *33*, 404–417. [\[CrossRef\]](#)
3. Groisman, P.Y.; Sherstyukov, B.G.; Razuvaev, V.N.; Knight, R.W.; Enloe, J.G.; Stroumentova, N.S.; Whitfield, P.H.; Førland, E.; Hannsen-Bauer, I.; Tuomenvirta, H.; et al. Potential forest fire danger over Northern Eurasia: Changes during the 20th century. *Glob. Planet. Chang.* **2007**, *56*, 371–386. [\[CrossRef\]](#)
4. Bowman, D.M.J.S.; Kolden, C.A.; Abatzoglou, J.T.; Johnston, F.H.; van der Werf, G.R.; Flannigan, M. Vegetation fires in the Anthropocene. *Nat. Rev. Earth Environ.* **2020**, *1*, 500–515. [\[CrossRef\]](#)
5. Roberts, K.E.; Lamoureux, S.F.; Kyser, T.K.; Muir, D.C.G.; Lafrenière, M.J.; Iqaluk, D.; Pieńkowski, A.J.; Normandeau, A. Climate and permafrost effects on the chemistry and ecosystems of High Arctic Lakes. *Sci. Rep.* **2017**, *7*, 13292. [\[CrossRef\]](#)
6. Gibson, C.M.; Chasmer, L.E.; Thompson, D.K.; Quinton, W.L.; Flannigan, M.D.; Olefeldt, D. Wildfire as a major driver of recent permafrost thaw in boreal peatlands. *Nat. Commun.* **2018**, *9*, 3041. [\[CrossRef\]](#)
7. Biskaborn, B.K.; Smith, S.L.; Noetzi, J.; Matthes, H.; Vieira, G.; Streletskiy, D.A.; Schoeneich, P.; Romanovsky, V.E.; Lewkowicz, A.G.; Abramov, A.; et al. Permafrost is warming at a global scale. *Nat. Commun.* **2019**, *10*, 264. [\[CrossRef\]](#)
8. Czerniawska, J.; Chlachula, J. Climate-Change Induced Permafrost Degradation in Yakutia, East Siberia. *Arctic* **2020**, *73*, 509–528. [\[CrossRef\]](#)

9. Heijmans, M.M.P.D.; Magnússon, R.Í.; Lara, M.J.; Frost, G.V.; Myers-Smith, I.H.; van Huissteden, J.; Jorgenson, M.T.; Fedorov, A.N.; Epstein, H.E.; Lawrence, D.M.; et al. Tundra vegetation change and impacts on permafrost. *Nat. Rev. Earth Environ.* **2022**, *3*, 68–84. [[CrossRef](#)]
10. MacDonald, G.M.; Velichko, A.A.; Kremenetski, C.V.; Borisova, O.K.; Goleva, A.A.; Andreev, A.A.; Cwynar, L.C.; Riding, R.T.; Forman, S.L.; Edwards, T.W.D.; et al. Holocene treeline history and climate change across Northern Eurasia. *Quat. Res.* **2000**, *53*, 302–311. [[CrossRef](#)]
11. Bigelow, N.H.; Brubaker, L.B.; Edwards, M.E.; Harrison, S.P.; Prentice, I.C.; Anderson, P.M.; Andreev, A.A.; Bartlein, P.J.; Christensen, T.R.; Cramer, W.; et al. Climate change and Arctic ecosystems: 1. Vegetation changes north of 55° N between the last glacial maximum, mid-Holocene, and present. *J. Geophys. Res.* **2003**, *108*, 8170. [[CrossRef](#)]
12. Andreev, A.A.; Klimanov, V.A. Quantitative Holocene climatic reconstruction from Arctic Russia. *J. Paleolimnol.* **2000**, *24*, 81–91. [[CrossRef](#)]
13. Andreev, A.A.; Tarasov, P.E.; Klimanov, V.A.; Melles, M.; Lisitsyna, O.M.; Hubberten, H.-W. Vegetation and climate changes around the Lama Lake, Taymyr Peninsula, Russia during the Late Pleistocene and Holocene. *Quat. Int.* **2004**, *122*, 69–84. [[CrossRef](#)]
14. Andreev, A.A.; Tarasov, P.E.; Siegert, C.; Ebel, T.; Klimanov, V.A.; Melles, M.; Bobrov, A.A.; Dereviagin, A.Y.; Lubinski, D.J.; Hubberten, H.-W. Late Pleistocene and Holocene vegetation and climate on the northern Taymyr Peninsula, Arctic Russia. *Boreas* **2003**, *32*, 484–505. [[CrossRef](#)]
15. Müller, S.; Tarasov, P.E.; Andreev, A.A.; Diekmann, B. Late Glacial to Holocene environments in the present-day coldest region of the Northern Hemisphere inferred from a pollen record of Lake Billyakh, Verkhoyansk Mts, NE Siberia. *Clim. Past.* **2009**, *5*, 73–84. [[CrossRef](#)]
16. Liu, S.; Stoof-Leichsenring, K.R.; Kruse, S.; Pestryakova, L.A.; Herzsuh, U. Holocene vegetation and plant diversity changes in the North-Eastern Siberian treeline region from pollen and sedimentary ancient DNA. *Front. Ecol. Evol.* **2020**, *8*, 560243. [[CrossRef](#)]
17. Novenko, E.Y.; Rudenko, O.V.; Mazei, N.G.; Kupriyanov, D.A.; Batalova, V.A.; Volkova, E.M.; Phelps, L.N.; Davis, B.A.S. Late-Holocene vegetation and fire history in Western Putorana Plateau (subarctic Siberia, Russia). *Holocene* **2022**, *32*, 433–441. [[CrossRef](#)]
18. Kobe, F.; Hoelzmann, P.; Gliwa, J.; Olschewski, P.; Peskov, S.A.; Shchetnikov, A.A.; Danukalova, G.A.; Osipova, E.M.; Goslar, T.; Leipe, C.; et al. Lateglacial–Holocene environments and human occupation in the Upper Lena region of Eastern Siberia derived from sedimentary and zooarchaeological data from Lake Ochaul. *Quat. Int.* **2022**, *623*, 139–158. [[CrossRef](#)]
19. Pestryakova, L.A.; Herzsuh, U.; Wetterich, S.; Ulrich, M. Present-day variability and Holocene dynamics of permafrost-affected lakes in central Yakutia (Eastern Siberia) inferred from diatom records. *Quat. Sci. Rev.* **2012**, *51*, 56–70. [[CrossRef](#)]
20. Nazarova, L.; Lüpfer, H.; Subetto, D.; Pestryakova, L.A.; Diekmann, B. Holocene climate conditions in central Yakutia (Eastern Siberia) inferred from sediment composition and fossil chironomids of Lake Temje. *Quat. Int.* **2013**, *290–291*, 264–274. [[CrossRef](#)]
21. Murton, J.B.; Edwards, M.E.; Lozhkin, A.V.; Anderson, P.M.; Savvinov, G.N.; Bakulina, N.; Bondarenko, O.V.; Cherepanova, M.V.; Danilov, P.P.; Boeskorov, V.; et al. Preliminary paleoenvironmental analysis of permafrost deposits at Batagaika megaslump, Yana uplands, northeast Siberia. *Quat. Res.* **2017**, *87*, 314–330. [[CrossRef](#)]
22. Feurdean, A.; Gałka, M.; Florescu, G.; Diaconu, A.-C.; Tant, I.; Kirpotin, S.; Hutchinson, S.M. 2000 years of variability in hydroclimate and carbon accumulation in western Siberia and the relationship with large-scale atmospheric circulation: A multi-proxy peat record. *Quat. Sci. Rev.* **2019**, *226*, 105948. [[CrossRef](#)]
23. Novenko, E.Y.; Mazei, N.G.; Kupriyanov, D.A.; Babeshko, K.V.; Kusilman, M.V.; Zyuganova, I.S.; Tsyganov, A.N.; Mazei, Y.A.; Phelps, L.N.; Davis, B.A. A 1300-year multi-proxy palaeoecological record from the northwest Putorana Plateau (Russian Subarctic): Environmental changes, vegetation dynamics and fire history. *Holocene* **2023**, *33*, 181–193. [[CrossRef](#)]
24. Clark, J.S.; Lynch, J.; Stocks, B.J.; Goldammer, J.G. Relationships between charcoal particles in air and sediments in west-central Siberia. *Holocene* **1998**, *8*, 19–29. [[CrossRef](#)]
25. De Groot, W.J.; Cantin, A.S.; Flannigan, M.; Soja, A.J.; Gowman, L.M.; Newbery, A. A comparison of Canadian and Russian boreal forest fire regimes. *For. Ecol. Manag.* **2013**, *294*, 23–34. [[CrossRef](#)]
26. Barhoumi, C.; Vogel, M.; Dugerdil, L.; Limani, H.; Joannin, S.; Peyron, O.; Ali, A.A. Holocene Fire Regime Changes in the Southern Lake Baikal Region Influenced by Climate-Vegetation-Anthropogenic Activity Interactions. *Forests* **2021**, *12*, 978. [[CrossRef](#)]
27. Glückler, R.; Herzsuh, U.; Kruse, S.; Andreev, A.; Vyse, S.A.; Winkler, B.; Biskaborn, B.K.; Pestrykova, L.; Dietze, E. Wildfire history of the boreal forest of south-western Yakutia (Siberia) over the last two millennia documented by a lake-sediment charcoal record. *Biogeosciences* **2021**, *18*, 4185–4209. [[CrossRef](#)]
28. Feurdean, A.; Diaconu, A.-C.; Pfeiffer, M.; Gałka, M.; Hutchinson, S.M.; Butiseaca, G.; Gorina, N.; Tonkov, S.; Niamir, A.; Tantau, I.; et al. Holocene wildfire regimes in forested peatlands in western Siberia: Interaction between peatland moisture conditions and the composition of plant functional types. *Clim. Past.* **2022**, *18*, 1255–1274. [[CrossRef](#)]
29. Novenko, E.Y.; Kupriyanov, D.A.; Mazei, N.G.; Prokushkin, A.S.; Phelps, L.N.; Buri, A.; Davis, B.A.S. Evidence that modern fires may be unprecedented during the last 3400 years in permafrost zone of Central Siberia, Russia. *Environ. Res. Lett.* **2022**, *17*, 025004. [[CrossRef](#)]
30. Chen, A.; Yang, L.; Sun, L.; Gao, Y.; Xie, Z. Holocene changes in biomass burning in the boreal Northern Hemisphere, reconstructed from anhydrosugar fluxes in an Arctic sediment profile. *Sci. Total Environ.* **2023**, *867*, 161460. [[CrossRef](#)]

31. Katz, N.Y. *Types of Bogs of the USSR and Western Europe and Their Geographical Distribution*; State Publishing House of Geographical Literature: Moscow, Russia, 1948.
32. Vasil'chuk, Y.; Vasil'chuk, A.; Budantseva, N.; Chizhova, J. *Palsa of Frozen Peat Mires*; Moscow University Press: Moscow, Russia, 2008.
33. Pyavchenko, N.I. *Bugristye Bolota*; Publishing House of the USSR Academy of Sciences: Moscow, Russia, 1955.
34. Levkovskaya, G.M.; Kind, N.B.; Zavel'ski, F.S.; Forova, V.S. The absolute age of peatlands in Igarka region and subdivision of the Holocene in West Siberia. *Bull. Comm. Study Quat.* **1970**, *37*, 94–101.
35. Beck, H.; Zimmermann, N.; McVicar, T.; Vergopolan, N.; Berg, A.; Wood, E.F. Present and future Köppen-Geiger climate classification maps at 1-km resolution. *Sci. Data* **2018**, *5*, 180214. [[CrossRef](#)] [[PubMed](#)]
36. Veselov, V.M.; Pribyl'skaya, I.P.; Mirzeabasov, O.A. *Nauchno-Prikladnoy Spravochnik "Klimat Rossii"*; Scientific and Applied Reference Book "Climate of Russia"; VNIIGMI-MCD: Obninsk, Russia, 2022. Available online: <http://aisori-m.meteo.ru/climsprn> (accessed on 1 May 2023).
37. Ershov, E.D. (Ed.) *Geocryologiya SSSR, Srednyaya Sibir*; Geocryology of USSR, Middle Siberia; Nedra-Press: Moscow, Russia, 1989.
38. Novenko, E.Y.; Mazei, N.G.; Prokushkin, A.S.; Kupryanov, D.A.; Shatunov, A.E.; Andreev, R.A.; Serikov, S.I. The Holocene palaeoecology of the palsa mire near Igarka (Yenisei Siberia). *IOP Conf. Ser. Earth Environ. Sci.* **2022**, *1093*, 012029. [[CrossRef](#)]
39. Novenko, E.Y.; Mazei, N.G.; Kupryanov, D.A.; Shatunov, A.E.; Andreev, R.A.; Makarova, E.A.; Borodina, K.A.; Rudenko, O.V. Vegetation changes in Yenisei Siberia over the last 4700 years: New palaeoecological data from Igarka area, Krasnoyarsk Region. *Geomorf. I Paleogeogr.* **2022**, *53*, 51–60.
40. Sokolov, S.Y.; Svyazeva, O.A.; Kubli, V.A. *Arealy Derev'ev i Kustarnikov SSSR [Areal of Trees and Shrubs of USSR]*; Nauka-Press Leningrad Branch: Leningrad, Russia, 1977; Volume 1.
41. Blaauw, M.; Christen, J.A. Flexible paleoclimate age-depth models using an autoregressive gamma process. *Bayesian Anal.* **2011**, *6*, 457–474. [[CrossRef](#)]
42. R Core Team. *R: A Language and Environment for Statistical Computing*; R Foundation for Statistical Computing: Vienna, Austria, 2021. Available online: www.R-project.org/ (accessed on 10 July 2023).
43. Reimer, P.; Austin, W.E.N.; Bard, E.; Bayliss, A.; Blackwell, P.G.; Bronk Ramsey, C.; Butzin, M.; Edwards, R.L.; Friedrich, M.; Grootes, P.M.; et al. The Intcal20 Northern Hemisphere radiocarbon age calibration curve (0–55 cal kBP). *Radiocarbon* **2020**, *4*, 725–757. [[CrossRef](#)]
44. Moore, P.D.; Webb, J.A.; Collinson, M.E. *Pollen Analysis*; Blackwell: Oxford, UK, 1991.
45. Bennett, K.D.; Willis, K.J. *Pollen. Tracking Environmental Change Using Lake Sediments Volume 3: Terrestrial, Algal, and Siliceous Indicators*; Smol, J.P., Birks, H.J., Last, W.M., Bradley, R.S., Alverson, K., Eds.; Springer: Dordrecht, The Netherlands, 2002; pp. 5–32.
46. Mazei, N.G.; Novenko, E.Y. The use of propionic anhydride in the sample preparation for pollen analysis. *Nat. Conserv. Res.* **2021**, *6*, 110–112. [[CrossRef](#)]
47. Stockmarr, J. Tablets with spores used in absolute pollen analysis. *Pollen Et Spores* **1971**, *1*, 615–621.
48. Reille, M. *Pollen Et Spores d'Europe Et d'Afrique Du Nord*; Laboratoire de Botanique Historique et Palynologie: Marseille, France, 1992.
49. Beug, H.-J. *Leitfaden der Pollenbestimmung für Mitteleuropa und Angrenzende Gebiete*; Verlag Friedrich Pfeil: Munich, Germany, 2004.
50. Van Geel, B. A palaeoecological study of Holocene peat bog sections in Germany and the Netherlands, based on the analysis of pollen, spores and macro- and microscopic remains of fungi, algae cormophytes and animals. *Rev. Palaeobot. Palynol.* **1978**, *25*, 1–120. [[CrossRef](#)]
51. Shumilovskikh, L.S.; Schlütz, F.; Achterberg, I.; Bauerochse, A.; Leuschner, H.H. Nonpollen palynomorphs from mid-Holocene peat of the raised bog Borsteler Moor (Lower Saxony, Germany). *Stud. Quat.* **2015**, *32*, 5–18.
52. Shumilovskikh, L.S.; Shumilovskikh, E.S.; Schlütz, F.; van Geel, B. NPP-ID: Non-Pollen Palynomorph Image Database as a research and educational platform. *Veget. Hist. Archaeobot.* **2022**, *31*, 323–328. [[CrossRef](#)]
53. Clark, R.L. Point count estimation of charcoal in pollen preparations and thin sections of sediments. *Pollen Spores* **1982**, *24*, 523–535.
54. Grimm, E. TILIA and TILIA*GRAPH.PC spreadsheet and graphics software for pollen data. *INQUA Work. Group Data-Handl. Methods Newsl.* **1990**, *4*, 5–7.
55. Benkova, V.E.; Schweingruber, F.H. *Anatomy of Russian Woods. An Atlas for the Identification of Trees, Shrubs, Dwarf Shrubs and Woody Lianas from Russia*; Haupt Verlag: Bern, Switzerland, 2004.
56. Mooney, S.; Tinner, W. The analysis of charcoal in peat and organic sediments. *Mires Peat* **2011**, *7*, 1–18.
57. Finsinger, W.; Bonnici, I. Tapas: An R Package to Perform Trend and Peaks Analysis. 2022. Available online: <https://zenodo.org/records/6344463> (accessed on 11 August 2023).
58. Overpeck, J.T.; Webb, T., III; Prentice, I.C. Quantitative interpretation of fossil pollen spectra: Dissimilarity coefficients and the method of modern analogs. *Quat. Res.* **1985**, *23*, 87–108. [[CrossRef](#)]
59. Guiot, J. Methodology of the last climatic cycle reconstruction in France from pollen data. *Palaeogeogr. Palaeoclim. Palaeoecol.* **1990**, *80*, 49–69. [[CrossRef](#)]
60. Nakagawa, T.; Tarasov, P.; Kotoba, N.; Gotanda, K.; Yasuda, Y. Quantitative pollen-based climate reconstruction in Japan: Application to surface and late Quaternary spectra. *Quat. Sci. Rev.* **2002**, *21*, 2099–2113. [[CrossRef](#)]

61. Williams, J.W.; Shuman, B. Obtaining accurate and precise environmental reconstructions from the modern analogue technique and North American surface pollen dataset. *Quat. Sci. Rev.* **2008**, *27*, 669–687. [[CrossRef](#)]
62. Chevalier, M.; Davis, B.A.S.; Heiri, O.; Seppä, H.; Chase, B.M.; Gajewski, K.; Lacourse, T.; Telford, R.J.; Finsinger, W.; Guiot, J.; et al. Pollen-based climate reconstruction techniques for late Quaternary studies. *Earth-Sci. Rev.* **2020**, *210*, 103384. [[CrossRef](#)]
63. Simpson, G.L.; Oksanen, J. Analogue: Analogue and Weighted Averaging Methods for Palaeoecology. R Package Version 0.17-6. 2021. Available online: <https://cran.r-project.org/package=analogue> (accessed on 5 August 2023).
64. Davis, B.A.S.; Chevalier, M.; Sommer, P.; Carter, V.A.; Finsinger, W.; Mauri, A.; Phelps, L.N.; Zanon, M.; Abegglen, R.; Åkesson, C.M.; et al. The Eurasian Modern Pollen Database (EMPD), version 2. *Earth Syst. Sci. Data* **2020**, *12*, 2423–2445. [[CrossRef](#)]
65. Ter Braak, C. Ordination. In *Data Analysis in Community and Landscape Ecology*; Jongman, R., Ter Braak, C., Van Tongeren, O., Eds.; Pudoc: Wageningen, The Netherlands, 1995; pp. 91–173.
66. Borren, W.; Bleuten, W.; Lapshina, E.D. Holocene peat and carbon accumulation rates in the southern taiga of Western Siberia. *Quat. Res.* **2004**, *61*, 42–51. [[CrossRef](#)]
67. Budantseva, N.A.; Chizhova, J.N.; Bludushkina, L.B.; Vasil'chuk, Y.K. Stable isotopes of oxygen, hydrogen and carbon and the age of palsas near the village of Yeletsky, north-east of the Bolshezemelskaya tundra. *Arctic. Antarctic.* **2017**, *4*, 38–56. [[CrossRef](#)]
68. Carcaillet, C.; Ali, A.A.; Blarquez, O.; Genries, A.; Mourier, B.; Bremond, L. Spatial variability of fire history in subalpine forests: From natural to cultural regimes. *Écoscience* **2009**, *16*, 1–12. [[CrossRef](#)]
69. Niemeyer, B.; Klemm, J.; Pstryakova, L.A.; Herzsuh, U. Relative pollen productivity estimates for common taxa of the northern Siberian Arctic. *Rev. Palaeobot. Palynol.* **2015**, *221*, 71–82. [[CrossRef](#)]
70. Klemm, J.; Herzsuh, U.; Pisaric, M.F.J.; Telford, R.J.; Heim, B.; Pstryakova, L.A. A pollen-climate transfer function from the tundra and taiga vegetation in Arctic Siberia and its applicability to a Holocene record. *Palaeogeog. Palaeoclimat. Palaeoecol.* **2013**, *386*, 702–713. [[CrossRef](#)]
71. Lopatina, D.A.; Zanina, O.G. Subrecent spore and pollen spectra from the Lower Kolyma River basin and their significance for reconstruction of Quaternary paleogeography of the region. *Stratigr. Geol. Correl.* **2016**, *24*, 103–105. [[CrossRef](#)]
72. Raschke, E.A.; Savelieva, L.A. Subrecent Spore-Pollen Spectra and Modern Vegetation from the Lena River Delta, Russian Arctic. *Contemp. Probl. Ecol.* **2017**, *4*, 456–472. [[CrossRef](#)]
73. Novenko, E.Y.; Mazei, N.G.; Kupriyanov, D.A.; Filimonova, L.V.; Lavrova, N.B. Subfossil Spore–Pollen Spectra from Larch Forests of Central Evenkia: Special Aspects of Interpretation for Paleoecological Research Purposes. *Russ. J. Ecol.* **2021**, *52*, 429–437. [[CrossRef](#)]
74. Malyshev, L.I.; Peshkova, G.A. (Eds.) *Flora of Central Siberia*; Nauka-Press, Siberian Branch: Novosibirsk, Russia, 1979.
75. Hantemirov, R.M.; Corona, C.; Guillet, S.; Shiyatov, S.G.; Stoffel, M.; Osborn, T.J.; Melvin, T.M.; Gorlanova, L.A.; Kukarskih, V.V.; Surkov, A.Y.; et al. Current Siberian heating is unprecedented during the past seven millennia. *Nat. Commun.* **2022**, *13*, 4968. [[CrossRef](#)]
76. Klemm, J.; Herzsuh, U.; Pstryakova, L.A. Vegetation, climate and lake changes over the last 7000 years at the boreal treeline in north-central Siberia. *Quat. Sci. Rev.* **2016**, *147*, 422–434. [[CrossRef](#)]
77. Kostrova, S.S.; Biskaborn, B.K.; Pstryakova, L.A.; Fernandoy, F.; Lenz, M.M.; Meyer, H. Climate and environmental changes of the Lateglacial transition and Holocene in northeastern Siberia: Evidence from diatom oxygen isotopes and assemblage composition at Lake Emanda. *Quat. Sci. Rev.* **2021**, *259*, 106905. [[CrossRef](#)]
78. Kharuk, V.I.; Ponomarev, E.I.; Ivanova, G.A.; Dvinskaya, M.L.; Coogan, S.C.P.; Flannigan, M.D. Wildfires in the Siberian taiga. *Ambio* **2021**, *50*, 1953–1974. [[CrossRef](#)] [[PubMed](#)]
79. Solomina, O.N.; Bradley, R.S.; Hodgson, D.A.; Ivy-Ochs, S.; Jomelli, V.; Mackintosh, A.N.; Nesje, A.; Owen, L.A.; Wanner, H.; Wiles, G.C.; et al. Holocene glacier fluctuations. *Quat. Sci. Rev.* **2015**, *111*, 9–34. [[CrossRef](#)]
80. Berger, A.; Loutre, M.F. Insolation values for the climate of the last 10 million years. *Quat. Sci. Rev.* **1991**, *10*, 297–317. [[CrossRef](#)]
81. Molinari, C.; Lehsten, V.; Blarquez, O.; Carcaillet, C.; Davis, B.A.S.; Kaplan, J.O.; Clear, J.; Bradshaw, R.H.W. The climate, the fuel and the land use: Long-term regional variability of biomass burning in boreal forests. *Glob. Chang. Biol.* **2018**, *24*, 4929–4945. [[CrossRef](#)] [[PubMed](#)]
82. Dvornikov, Y.; Novenko, E.; Korets, M.; Olchev, A. Wildfire Dynamics along a North-Central Siberian Latitudinal Transect Assessed Using Landsat Imagery. *Remote Sens.* **2022**, *14*, 790. [[CrossRef](#)]
83. Knorre, A.; Kirdeyanov, A.; Prokushkin, A.; Krusic, P.; Büntgen, U. Tree ring-based reconstruction of the long-term influence of wildfires on permafrost active layer dynamics in Central Siberia. *Sci. Total Environ.* **2019**, *652*, 314–319. [[CrossRef](#)] [[PubMed](#)]
84. Self, A.E.; Jones, V.J.; Brooks, S.J. Late Holocene environmental change in arctic western Siberia. *Holocene* **2015**, *25*, 150–165. [[CrossRef](#)]
85. Kumke, T.; Kienel, U.; Weckström, J.; Korhola, A.; Hubberten, H.-W. Inferred Holocene Paleotemperatures from Diatoms at Lake Lama, Central Siberia. *Arct. Antarct. Alp. Res.* **2004**, *36*, 624–634. [[CrossRef](#)]
86. Christiansen, B.; Ljungqvist, F.C. The extra-tropical Northern Hemisphere temperature in the last two millennia: Reconstructions of low-frequency variability. *Clim. Past* **2012**, *8*, 765–786. [[CrossRef](#)]

87. PAGES 2k Consortium. Consistent multidecadal variability in global temperature reconstructions and simulations over the Common Era. *Nat. Geosci.* **2019**, *12*, 643–649. [[CrossRef](#)]
88. Rudenko, O.; Taldenkova, E.; Ovsepyan, Y.; Stepanova, A.; Bauch, H.A.A. Multiproxy-based reconstruction of the mid- to late Holocene paleoenvironment in the Laptev Sea off the Lena River Delta (Siberian Arctic). *Palaeogeog. Palaeoclimat. Palaeoecol.* **2020**, *540*, 109502. [[CrossRef](#)]

Disclaimer/Publisher’s Note: The statements, opinions and data contained in all publications are solely those of the individual author(s) and contributor(s) and not of MDPI and/or the editor(s). MDPI and/or the editor(s) disclaim responsibility for any injury to people or property resulting from any ideas, methods, instructions or products referred to in the content.